Persistent quantum interfering electron trajectories

J. E. Kruse,[1,2] P. Tzallas,[1,*] E. Skantzakis,[1,2] and D. Charalambidis[1,2]

[1]*Foundation for Research and Technology—Hellas, Institute of Electronic Structure and Laser, Post Office Box 1527, 7GR-1110 Heraklion, Crete, Greece*

[2]*Department of Physics, University of Crete, Post Office Box 2208, GR-71003 Heraklion, Crete, Greece*

(Received 7 June 2010; published 30 September 2010)

The emission of above-ionization-threshold harmonics results from the recombination of two-electron wave packets moving along a "short" and a "long" trajectory in the atomic continuum. Attosecond pulse train generation has, so far, been attributed to the short trajectory, attempted to be isolated through targeted trajectory-selective phase-matching conditions. Here, we provide experimental evidence for the contribution of both trajectories to the harmonic emission, even under phase-matching conditions unfavorable for the long trajectory. This is finger printed in the interference modulation of the harmonic yield as a function of the driving laser intensity. The effect is also observable in the sidebands, which arise from the frequency mixing of the harmonics and the driving laser field, an effect with consequences in cross-correlation pulse metrology approaches.

DOI: 10.1103/PhysRevA.82.033438 PACS number(s): 32.80.Rm, 42.65.Ky, 42.50.Hz, 42.65.Re

I. INTRODUCTION

Harmonic generation above the ionization threshold is governed by the recombination of localized electron wave packets ejected into the continuum and driven back toward the core upon reversal of the linearly polarized driving field [1]. According to this model, at a given driving laser intensity I_L, two quantum interfering electron trajectories (QIET) with two different total flight times $\tau_q^L(I_L)$ and $\tau_q^S(I_L)$ contribute to the emission of each harmonic q. L and S stand for long and short [1]. The electron wave-packet phases, accumulated during their motion in the continuum, and with it the phases of the emitted harmonics, approximated by $\varphi_q^{L,S}(I_L) \approx -U_p \tau_q^{L,S}(I_L)$ (where U_p is the ponderomotive energy) are proportional to the product $\tau_q^{L,S}(I_L) I_L$ [1]. The driving-intensity-dependent phase difference of the two trajectories $\Delta\varphi_q^{L,S}(I_L) = \varphi_q^L(I_L) - \varphi_q^S(I_L) \propto [\tau_q^L(I_L) - \tau_q^S(I_L)] I_L \neq 0$ leads to alternating constructive and destructive interference. This results in a modulation of the harmonic yield $Y_q(I_L) \propto |E_q^S e^{-i(\omega_q t + \varphi_q^S(I_L))} + E_q^L e^{-i(\omega_q t + \varphi_q^L(I_L))}|^2$. As the driving laser intensity I_L increases, the difference in flight times $\Delta\tau_q^{L,S}(I_L) = \tau_q^L(I_L) - \tau_q^S(I_L)$ increases more rapidly. This results in a reduction of the period of the harmonic yield's modulation. On the other hand, for higher harmonic orders q, the difference in flight time $\Delta\tau_q^{L,S}$ is shorter, resulting in a slower modulation of the harmonic yield. Figure 1(a) shows the dependence of $\Delta\varphi_q^{L,S}(I_L)$ (for $13 \leqslant q \leqslant 17$) on the intensity of the driving laser field, calculated by solving of the quantum-mechanical three-step model [1]. For plateau harmonics the intensity dependence of $\Delta\varphi_q^{L,S}$ is close to linear, but when the harmonics are close to the cutoff region (in the present case the 17th harmonic) it becomes nonlinear. $\Delta\varphi_q^{L,S}$ stays close to zero, for above cutoff harmonics. This behavior can be seen in Fig. 1(b) which shows the dependence of $d(\Delta\varphi_q^{L,S}(I_L))/dI_L$ on the driving laser intensity. The so-far discussed atomic response leads to the emission of harmonic radiation that is further modified through propagation in the generating medium, which affects the emitted yield through phase matching. The condition for optimal phase matching of focused Gaussian beams is $\vec{k}_q = q\vec{k} + \Delta\vec{k}_g + \Delta\vec{k}_d + \vec{\nabla}\varphi_q^{L,S}$ with $\vec{k}_q$ and $\vec{k}$ being the k vectors of the qth harmonic and the fundamental, respectively, $\Delta\vec{k}_g$ the Gouy phase, and $\Delta\vec{k}_d$ the mismatch caused through dispersion [1]. This condition favors far off-axis generation by the long trajectory and on-axis generation by the short trajectory, only if the laser focus is before the jet [2,3]. For this reason, interference effects have been mostly studied in detail for off-axis harmonic generation [4]. In the present work we demonstrate on-axis interference of the two trajectories for all three focus positions, namely the focus before, on, and after the gas jet. These are also the conditions under which the effect was, so far, not expected. The observed interference manifests the contribution of both trajectories in all three geometries, even though with different weighting factors [5]. The interference effect has recently been observed also on-axis for *below-threshold* harmonic generation at the focus [6].

II. EXPERIMENTAL SETUP

The experiments have been conducted using the FORTH-ULF 4TW Ti:sapphire laser system delivering pulses of 40 fs duration at 10 Hz, central wavelength 800 nm, and energy of up to 150 mJ/pulse. The experimental setup used in the present study is described in detail in Refs. [5,7]. A mask with a hole in the center was placed in the laser beam to create a 1.5 mm diameter IR beam (dressing-beam) in the center of an annular beam, which was focused by a lens of 3 m focal length into a pulsed xenon gas jet of $\approx$700 μm length and an estimated atomic density of $10^{16}-10^{17}$ atoms/cm^3, where the odd harmonics were generated. The temporal delay between the dressing-beam and annular beam was zero. After the Xe jet a silicon wafer was placed at the fundamentals Brewster angle of 75° to reduce the IR radiation and to reflect the harmonics [8] toward the detection area. A $\lambda/2$ wave plate was used to rotate the polarization of the laser by a very small angle (<3°) in order for a small fraction of the central IR dressing-beam to be reflected by the wafer toward the detection area. The reflected

*Corresponding author: ptzallas@iesl.forth.gr

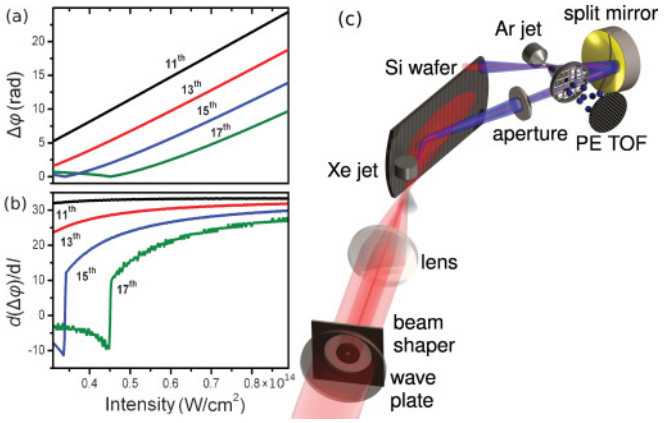

FIG. 1. (Color online) (a) and (b) Calculated dependence of $\Delta\varphi_q^{\mathrm{L,S}}$ (for $13 \leqslant q \leqslant 17$) and $d(\Delta\varphi_q^{\mathrm{L,S}}(I_{\mathrm{L}}))/dI_{\mathrm{L}}$, respectively, on the intensity of the driving laser field. (c) Schematic of the experimental setup.

two-color beam passed through a 2 mm diameter aperture, placed 2 m downstream from the Xe jet, which was blocking further any residual part of the annular IR radiation and was selecting only the central part of the beam cross section. Then the beam was focused by a gold-coated spherical mirror of 5 cm focal length into an argon pulsed gas jet. For the measurement of the interference effect between the two-electron trajectories, photoelectron (PE) spectra of argon, ionized in the presence of the XUV and IR field, have been recorded as a function of the laser field intensity. The PE spectra consist of a series of 11th–17th harmonic single-photon ionization peaks and additional two-photon ionization (XUV $\pm$ IR) "sideband" peaks S12–S16 appearing between them. The intensity of the laser at the harmonic generation region was varied between $\approx 4 \times 10^{13}$ and $\approx 10^{14}$ W/cm^2. Measurements have been performed for three different positions of the laser focus with respect to the position of the gas jet, (I) $z_{\mathrm{BJ}} = -0.43b$ (laser focus before jet), (II) $z_{\mathrm{OJ}} = 0$ (laser focus at jet), and (III) $z_{\mathrm{AJ}} = +0.28b$ (laser focus after jet), respectively. $b = 18$ cm is the confocal parameter, assuming Gaussian beam geometry. It is known from modeling, including propagation effects in the generating medium [2], that phase matching favors in case (I) the contribution of the short trajectory, in case (II) both, and in case (III) the contribution of the long trajectory to the harmonic emission. In our case, the contribution of the long trajectory has been further reduced by the on-axis spatial filtering mentioned previously.

III. RESULTS AND DISCUSSION

Figure 2 shows the measured signal from the PE peaks of the 13th and 15th harmonic ionization and from the S12–S16 sidebands in dependence on the laser intensity for the three positions of the laser focus. The upper panel shows an example of raw data points (gray dots) of harmonic 13 together with a 10 points moving average over the raw data (red line). A low contrast modulation is observable superimposed on a steadily, nonlinearly increasing "background." The middle and lower panels show the measured modulation for harmonics 13th and 15th and sidebands S12–S16 after dividing with the steadily increasing "background" for all three geometries. In all cases

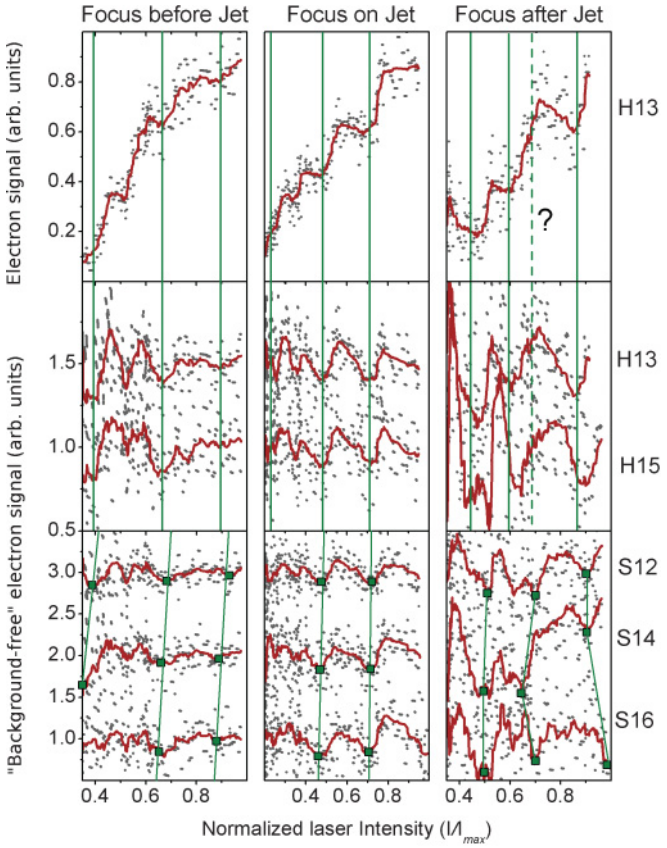

FIG. 2. (Color online) Measured dependence of the 13th and 15th harmonic and the S12–S16 sidebands on the laser intensity for the three positions of the laser focus. Upper panel: Arbitral example of raw data points (gray dots) of harmonic 13th together with a 10 points moving average of the raw data (red line). Middle and lower panel: Measured modulation of the harmonics 13th and 15th and the S12–S16, respectively, are shown after removing the steadily increasing "background" for all three geometries.

the measured signals present the following characteristic features.

(1) They feature an oscillatory modulation, with double peak interference maxima. This is more pronounced when focusing before the jet and at the jet. The periods of the oscillations are $0.27 \times I_{\mathrm{max}}$ and $0.23 \times I_{\mathrm{max}}$ when focusing before the jet and $0.25 \times I_{\mathrm{max}}$ and $0.23 \times I_{\mathrm{max}}$ when focusing at the jet. The average period of the oscillations is $\approx 0.23 \times I_{\mathrm{max}}$, which corresponds to an oscillation period of $\approx 0.23 \times 10^{14}$ W/cm^2 for $I_{\mathrm{max}} \approx 10^{14}$ W/cm^2. This is in reasonable agreement with the expected value of 0.3×10^{14} W/cm^2 [1,4].

(2) The distance between the maxima or minima (green lines in Fig. 2) when focusing before and at the jet becomes smaller for higher laser intensities, in agreement with the theoretical predictions given in Figs. 1(a) and 1(b). When focusing after the jet this behavior is not observed. This could be due to the not-observed double minima structure, leading to an uncertainty whether an observed minimum is a "main" or a "secondary" one.

(3) The fringe contrast, which depends on the percentage of the long trajectory contribution, becomes higher as the focus moves from before to after the jet. The harmonic and sideband

fringe contrast, when focusing before, at, and after the jet, is ≈9%, ≈12%, and ≈25%, respectively.

(4) From one sideband to the next, the positions of the interference minima shift. This magnitude of the shift, which is illustrated by the tilted green lines in the lower panels of Fig. 2, depends on the intensity of the driving laser field, the sideband order, and the focusing geometry. When focusing before or at the jet, the interference minima are shifted to lower laser intensities for the higher sideband orders. The effect is stronger when focusing before the jet. When focusing after the jet no systematic shifts have been observed. This could relate to the sensitivity of the long trajectories on the variations of the driving laser intensity.

(5) Interestingly, even the harmonics close to the cutoff region (like the 17th) show an interference modulation. This observation, shown in the modulation of the signal of the S16 in Fig. 2, is compatible with the results of the quantum-mechanical three-step model, according to which both trajectories are contributing to the cutoff harmonics, but the difference $(\tau_{\mathrm{cutoff,L}} - \tau_{\mathrm{cutoff,S}})$ is much smaller than for plateau harmonics. This is manifested in the observed long modulation intervals clearly seen for the lower intensities in Fig. 3.

Considering both the short and long trajectories contributing to the harmonic generation process, the modulation of the sideband signal (S_{q+1}) [the index $(q+1)$ indicates the order of the sideband] with the laser intensity I_{L} and delay τ reads

$$S_{q+1}(\tau, I_{\mathrm{L}}) \propto \cos\left(2\omega_{\mathrm{L}}\tau + \Delta\varphi^{\mathrm{S}}_{q,q+2}\right) + \cos\left(2\omega_{\mathrm{L}}\tau + \Delta\varphi^{\mathrm{L}}_{q,q+2}\right) + 2\cos(A_{q+1})\cos\left(2\omega_{\mathrm{L}}\tau + \frac{\Delta\varphi^{\mathrm{S}}_{q,q+2} + \Delta\varphi^{\mathrm{L}}_{q,q+2}}{2}\right) + \cos\left(\Delta\varphi^{\mathrm{SL}}_{q}\right) + \cos\left(\Delta\varphi^{\mathrm{SL}}_{q+2}\right), \quad (1)$$

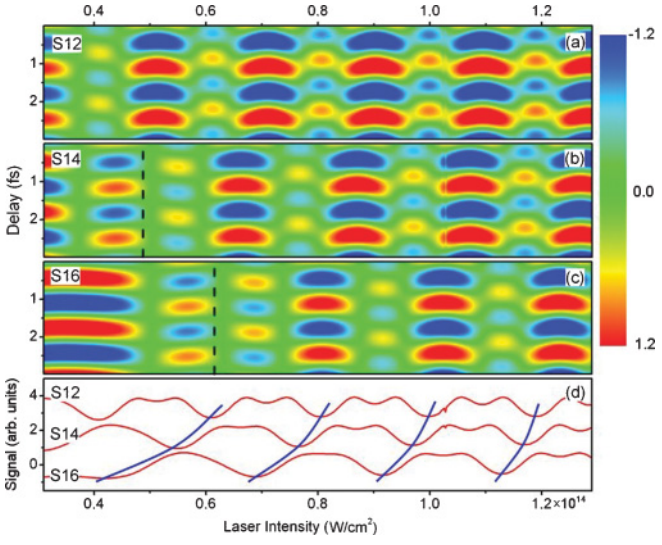

FIG. 3. (Color online) (a), (b), and (c) Calculated modulation of the sidebands S12–S16 as a function of the delay τ and the laser intensity (I_{L}). (d) A line-out of Figs. 3(a), 3(b), and 3(c) at $\tau = 2.67$ fs (equivalent to zero delay between XUV and IR) shows the sideband signal as a function of I_{L}.

where $A_{q+1} = \frac{1}{2}(\Delta\varphi^{\mathrm{SL}}_{q} + \Delta\varphi^{\mathrm{SL}}_{q+2})$, $\Delta\varphi^{\mathrm{S}}_{q,q+2} = \varphi^{\mathrm{S}}_{q} - \varphi^{\mathrm{S}}_{q+2}$, $\Delta\varphi^{\mathrm{L}}_{q,q+2} = \varphi^{\mathrm{L}}_{q} - \varphi^{\mathrm{L}}_{q+2}$, $\Delta\varphi^{\mathrm{SL}}_{q} = \varphi^{\mathrm{S}}_{q} - \varphi^{\mathrm{L}}_{q}$, and $\Delta\varphi^{\mathrm{SL}}_{q+2} = \varphi^{\mathrm{S}}_{q+2} - \varphi^{\mathrm{L}}_{q+2}$. Here φ^{S}_{q} and φ^{L}_{q} are the phases of harmonics generated by electrons from the short and long trajectory, respectively, and ω_{L} is the fundamental laser frequency. In Eq. (1) the atomic phase shift is assumed to be zero due to its negligible influence on the sideband signal. Further, it is assumed that the harmonic intensity does not depend on the laser intensity, and that $I^{\mathrm{S}}_{q} = I^{\mathrm{L}}_{q} = I^{\mathrm{S}}_{q+2} = I^{\mathrm{L}}_{q+2}$, which are the normalized intensities of the harmonic orders q or $q+2$ generated by the short or long trajectories, respectively. The phases of the harmonics were calculated from the quantum-mechanical version of the three-step model [1]. Propagation effects in the harmonic generation medium were not taken into account. Figures 3(a), 3(b), and 3(c) show the modulation of the sideband signal S12–S16 as a function of the delay τ and the laser intensity (I_{L}). The dashed lines depict the intensity values where the harmonics contributing to the sideband $q+1$ reach the cutoff. Figure 3(d) shows the line outs of Figs. 3(a), 3(b), and 3(c) at $\tau = 2.67$ fs (2π delay between XUV and IR) to illustrate the dependence of the sideband signal on I_{L} at the experimental conditions of the present work. The blue lines in Fig. 3(d) connect the positions of the interference minima between the sidebands. All characteristic features (1)–(5) of the experimental results shown in Fig. 2 are in reasonable agreement with the calculated ones shown in Fig. 3(d):

(1) An oscillatory modulation with double peak interference maxima has been calculated.

(2) The distance between the maxima or minima becomes smaller at higher laser intensities.

(3) The fringe contrast (not shown in the calculations) depends on the percentage of the long trajectory contribution.

(4) The relative position of the interference minima or maxima between the different sidebands (blue lines) depends on the intensity of the driving laser field and the sideband order.

(5) The harmonics close to the cutoff region show an interference modulation.

The shift to lower laser intensities of the sideband interference minima is more pronounced in the calculated than in the measured trace, which could be attributed to propagation effects that are not taken into account in the calculations. The intensity dependence of the harmonic phase further results in an intensity dependence of the pulse duration in the attosecond pulse train. Due to the stronger intensity dependence of the long trajectory's phase, a driving intensity variation may lead to destruction of the attosecond confinement, when both trajectories contribute to the XUV emission. On-axis harmonic generation by laser beams focused before the gas jet was, so far, considered to eliminate the long trajectory. The present findings, in agreement with those of our relevant recent work [5] on a comparative study between the second-order intensity volume autocorrelation (IVAC) [9] and the reconstruction of attosecond beating by interference of two-photon transitions (RABITT) [10] technique, do not sustain this assumption, evidencing implications to the emitted pulse durations and their metrology.

IV. CONCLUSION

We show that both the long and the short trajectories are contributing to on-axis harmonic generation in a gas medium. We show this for both plateau and cutoff harmonics, at different phase-matching conditions. Phase matching affects, to a certain degree, the relative contribution of the two trajectories, but it does not fully eliminate any of the two. The results of this work are in full agreement with pulse duration measurements of attosecond pulse trains through second-order IVAC [9], but in conflict with those conducted with the RABITT approach [10]. Thus, they play a significant role for the accuracy of measuring attosecond pulses by means of cross-correlation techniques. They further contribute to the improvement of the accuracy of atomic-molecular tomography techniques [11] and precision measurements with frequency combs in the XUV spectral region [6,12]. An on-axis QIET scan in such experiments can be used to assess the presence of the long trajectory contribution.

ACKNOWLEDGMENTS

This work was supported, in part, by the Ultraviolet Laser Facility (ULF) operating at FORTH-IESL (Contract No. HPRI-CT-2001–00139), the ELI research infrastructure preparatory phase program, and the FASTQUAST ITN (Contract No. CA-ITN-214962).

[1] P. B. Corkum, Phys. Rev. Lett. **71**, 1994 (1993); K. J. Schafer, B. Yang, L. F. DiMauro, and K. C. Kulander, *ibid.* **70**, 1599 (1993); M. Lewenstein, P. Balcou, M. Y. Ivanov, A. L'Huillier, and P. B. Corkum, Phys. Rev. A **49**, 2117 (1994); M. Lewenstein, P. Salieres, and A. L'Huillier, *ibid.* **52**, 4747 (1995); P. Salieres *et al.*, Science **292**, 902 (2001); P. Balcou, P. Salieres, A. L'Huillier, and M. Lewenstein, Phys. Rev. A **55**, 3204 (1997).

[2] M. B. Gaarde and K. J. Schafer, Phys. Rev. Lett. **89**, 213901 (2002); P. Antoine, A. L'Huillier, and M. Lewenstein, *ibid.* **77**, 1234 (1996).

[3] M. Bellini, C. Lynga, A. Tozzi, M. B. Gaarde, T. W. Hansch, A. L'Huillier, and C. G. Wahlstrom, Phys. Rev. Lett. **81**, 297 (1998); P. Salieres, A. L'Huillier, and M. Lewenstein, *ibid.* **74**, 3776 (1995); H. Merdji, M. Kovacev, W. Boutu, P. Salieres, F. Vernay, and B. Carre, Phys. Rev. A **74**, 043804 (2006).

[4] A. Zaïr *et al.*, Phys. Rev. Lett. **100**, 143902 (2008); T. Auguste *et al.*, Phys. Rev. A **80**, 033817 (2009); G. Sansone, E. Benedetti, J. P. Caumes, S. Stagira, C. Vozzi, M. Pascolini, L. Poletto, P. Villoresi, S. DeSilvestri, and M. Nisoli, Phys. Rev. Lett. **94**, 193903 (2005); G. Sansone, E. Benedetti, J. P. Caumes, S. Stagira, C. Vozzi, S. DeSilvestri, and M. Nisoli, Phys. Rev. A **73**, 053408 (2006).

[5] J. E. Kruse *et al.*, Phys. Rev. A **82**, 021402(R) (2010).

[6] D. C. Yost *et al.*, Nat. Phys. **5**, 815 (2009).

[7] O. Faucher *et al.*, Appl. Phys. B **97**, 505 (2009).

[8] E. J. Takahashi *et al.*, Opt. Lett. **29**, 507 (2004).

[9] P. Tzallas *et al.*, Nature (London) **426**, 267 (2003); L. A. A. Nikolopoulos, E. P. Benis, P. Tzallas, D. Charalambidis, K. Witte, and G. D. Tsakiris, Phys. Rev. Lett. **94**, 113905 (2005); Y. Nabekawa, T. Shimizu, T. Okino, K. Furusawa, H. Hasegawa, K. Yamanouchi, and K. Midorikawa, *ibid.* **96**, 083901 (2006); Y. Nomura *et al.*, Nature Phys. **5**, 124 (2009).

[10] P. M. Paul *et al.*, Science **292**, 1689 (2001); Y. Mairesse *et al.*, *ibid.* **302**, 1540 (2003); L. C. Dinu, H. G. Muller, S. Kazamias, G. Mullot, F. Auge, P. Balcou, P. M. Paul, M. Kovacev, P. Breger, and P. Agostini, Phys. Rev. Lett. **91**, 063901 (2003); S. A. Aseyev, Y. Ni, L. J. Frasinski, H. G. Muller, and M. J. J. Vrakking, *ibid.* **91**, 223902 (2003); Y. Mairesse and F. Quéré, Phys. Rev. A **71**, 011401(R) (2005).

[11] T. Remetter *et al.*, Nat. Phys. **2**, 323 (2006); J. Itatani *et al.*, Nature (London) **432**, 867 (2004); S. Haessler *et al.*, Nat. Phys. **6**, 200 (2010).

[12] C. Gohle *et al.*, Nature (London) **436**, 234 (2005).